A HYBRID BRAIN-COMPUTER INTERFACE FOR INTELLIGENT PROSTHETICS

A Thesis

by

YU-CHE CHENG

Submitted to the Office of Graduate and Professional Studies of
Texas A&M University
in partial fulfillment of the requirements for the degree of

MASTER OF SCIENCE

Chair of Committee,	Reza Langari
Committee Members,	Won-Jong Kim
	Dezhen Song
Head of Department,	Andreas Polycarpou

December 2014

Major Subject: Mechanical Engineering

ABSTRACT

Over the past few decades, many researchers have shown that humans can use brain signals to communicate with computers or machines by using brain-computer interfaces (BCIs). BCI systems can measure the brain activities and translate them into control signals to external devices. A hybrid BCI system integrates two or more different BCI systems. By combining two different BCIs, the disadvantages can be eliminated and the advantages can stay.

One of the BCI developed in this thesis is electroencephalographic (EEG). EEG is one of the imaging techniques for spontaneous recording of the electrical activity from the brain. The EEG has been widely used in researches for cognitive and brain-state studies in psychology, neuroprosthetics, transportation safety and clinical diagnosis . In this thesis a commercial EEG product, NeuroSky MindWave, is used to measure the EEG signals from the forehead. From the acquired EEG signals, humans attention and meditation level can be obtain and control an intelligent prosthesis. An EEG control algorithm is developed in LabVIEW based on the attention level, meditation level and eye blinks.

The other BCI used is eye-gaze tracking technology. Eye-gaze tracking technology is used to obtain the human's gaze direction. An eye-gaze tracking system is developed in this research. The system consists of a wearable self-build eye-gaze tracker with a scene camera and an eye-gaze tracking algorithm developed in LabVIEW, which can locate the eye pupil center and estimate the gaze direction.

Combining these two BCIs above, a hybrid BCI system is complete. This hybrid BCI can help a person with disabilities grab one specific item through an intelligent prosthetic arm. The eye-gaze tracker pinpoints the item that the person wants exactly, and EEG BCI controls the prosthetic arm to grasp the item. The hybrid BCI system is robust enough and has a reliable accuracy from the experimental result.

DEDICATION

To my dear family.

ACKNOWLEDGEMENTS

I would like to thank my committee chair, Dr. Langari, and my committee members, Dr. Kim and Dr. Song, for their guidance and support of this research.

Thanks also go to my friends and lab members and the department faculty and staff for insturcting me not only in research, but also in daily life. I also want to extend my gratitude to the National Instruments, which provided the LabVIEW software and Vision Development Module.

Finally, thanks to my parents for their encouragement and to my wife for her patience and love.

TABLE OF CONTENTS

Page

LIST OF FIGURES

Page

LIST OF TABLES

Page

CHAPTER I

INTRODUCTION

Research about Brain-computer interface (BCI) has been widely developed over the past few decades. The objective of BCI research is to establish a new communication system that translates human intentions into a control signal for an external device such as a computer, a assistive appliance or a neuroprosthesis (Wolpaw and others 2002, 767-791). Humans can send commands to such external devices directly without involvement of peripheral nerves and muscles. BCIs use signals recorded from the scalp, the surface of the cortex, or inside of the brain to enable users to communicate with computers or output devices. Nowadays, BCIs are widely used in various areas such as neuroscience, clinical diagnosis, rehabilitation, engineering, computer science, etc.

The basic concepts of a BCI contains five steps: signal acquisition, signal enhancement, feature extraction, classification, and the control interface. (Khalid and others 2009, 1-4) And there are several types of brain signals using in BCI such as electroencephalography (EEG), magnetoencephalography (MEG), positron emission tomography (PET), functional magnetic resonance imaging (fMRI), and optical imaging. (Wolpaw and others 2002, 767-791) The BCIs of MEG, PET, fMRI, and optical imaging are still technically demanding and expensive. Furthermore, PET, fMRI, and optical imaging, which depend on blood flow, have long time constants and thus are less amenable to rapid communication. In sum, only EEG and related methods require relatively simple, inexpensive and convenient equipment (Wolpaw and others 2002,

767-791). The comparison of different types of BCI is shown in Table 1 which modified from (Nicolas-Alonso and Gomez-Gil 2012, 1211-1279).

	Acitivity Measured	**Measurement**	**Temporal Resolution**	**Risk**	**Portability**
EEG	Electrical	Direct	~0.05s	Non-invasive	Portable
MEG	Magnetic	Direct	~0.05s	Non-invasive	Non-portable
ECoG	Electrical	Direct	~0.003s	Invasive	Portable
PET	Metabolic	Indirect	~0.01s	Non-invasive	Non-portable
fMRI	Metabolic	Indirect	~1s	Non-invasive	Non-portable

Table 1. Summary of common BCIs

Motivation

Nowadays, people who use prosthetic limbs become more and more. Most of the prosthetic limbs can be divided into four types: body-powered arms, lower extremity prosthetics, myoelectric and robotic prostheses. Only robotic prostheses above receive signals directly from human brain so BCIs are usually used to control them. Moreover, some neurodegenerative diseases such as Amyotrophic lateral sclerosis (ALS) can cause the patient loose muscle weakness and atrophy throughout the body. Due to muscle atrophy, the patients have such neurodegenerative diseases cannot control the body-powered arms, lower extremity prosthetics or myoelectric prostheses well. BCIs create a direct communicating method between brain and prosthesis which are widely utilized in the world.

The concept of a general BCI system is shown in Figure 1. Typically, there are two types of method to extract signals from the brain, Invasive BCIs, Non-invasive BCIs. These two types of BCIs are introduced below.

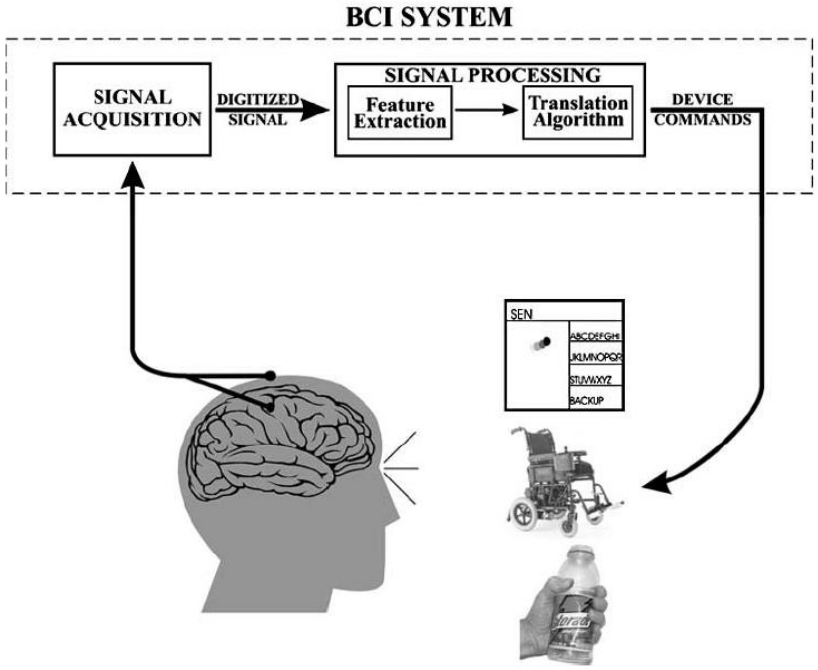

Figure 1. The concept of a general BCI system. (Schalk and others 2004, 1034-1043)

Invasive BCIs

Invasive BCIs need to implant electrodes into the cranium during the surgery. (Nicolas-Alonso and Gomez-Gil 2012, 1211-1279) The researchers implant chips which contains hundreds of microelectrodes into the cranium in order to record the signals generate from the neurons. At present, two types of invasive BCIs can be found: electrocorticography (ECoG) and intracortical neuron recording. ECoG places electrodes on the surface of the cortex and intracortical neuron recording puts the electrodes inside

the cortex. The invasive BCIs have the highest quality signals, however, they have the highest rick as well.

Non-invasive BCIs

The non-invasive BCIs measure the brain signals from outside of human body. Two types of brain signals can be measured: electrophysiological and hemodynamic. (Nicolas-Alonso and Gomez-Gil 2012, 1211-1279) Electrophysiological signals is generated by the thousands of neurons in the brain. Electrophysiological signals include electroencephalography (EEG), magnetoencephalography (MEG) and electrical signal acquisition in single neurons. Hemodynamic signals comes from measuring the change of the local ration of oxyhemoglobin to deoxyhemoglobin. Hemodynamic BCI can measure this change by functional magnetic resonance (fMRI) and near infrared spectroscopy. (Nicolas-Alonso and Gomez-Gil 2012, 1211-1279) Nowadays, EEG is the most popular non-invasive BCI. The EEG-based BCI is easy to use, portable and relative low cost. However, EEG signals suffer from a reduced spatial resolution and noise because the electrodes placed on the scalp which is not direct contact with the neurons. Generally speaking, EEG signals can reflect the electrical activities of millions of neurons under the scalp which is corresponding to the brain activities. (Zhang, Wang, and Fuhlbrigge 2010, 379-384). Figure 2 shows some invasive and non-invasive BCIs.

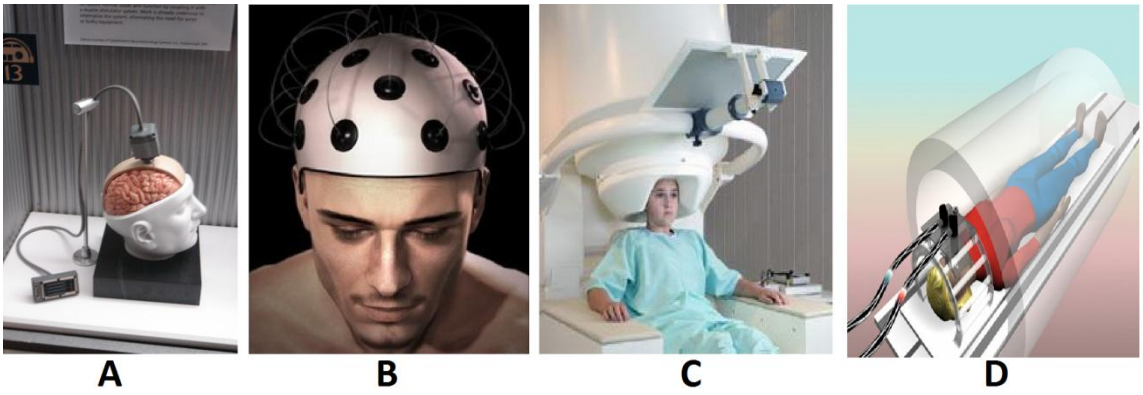

Figure 2. Types of invasive and non-invasive BCIs. (A) ECoG. (B) EEG. (C) MEG. (D) fMRI

Related Work

To enhance the performance of BCIs, the hybrid BCI system is proposed by Gert Pfurtscheller which use two different brain signals simultaneously (Pfurtscheller and others 2010). In this thesis, an EEG-based BCI will be combined with a gaze tracking technique as a hybrid BCI. Typical medical EEG devices cost more than $50,000 USD. However, some companies have made efforts to commercialize non-invasive EEG devices, especially for game industry or educational purpose. These devices translate the brain electrical signals into computer commands directly. Here three popular commercial EEG devices in the market will be introduced below.

Neural Impulse Actuator by OCZ

The Neural Impulse Actuator (NIA) is an EEG device developed by OCZ Technology. It has three electrodes on headband as shown in Figure 3. The NIA measures EEG signals of muscles, eyes and brain, respectively. It is designed for games

industry. The user can interact with computer via three method: eyebrow movement, eyeball movement or brain signal. It is not hard to using the eyebrow up/down to move paddle to up/down position with some training procedure. However, for the other two methods, it need more time to train and hard to control compare with eyebrow movement. (Zhang, Wang, and Fuhlbrigge 2010, 379-384)

Figure 3. OCZ neural impulse actuator.

Emotive EPOC and EPOC+

Emotiv EPOC and EPOC+ are the two generation EEG device developed by Emotiv Inc. The Emotiv EPOC is a high resolution, multi-channel, portable system which has been designed for EEG research applications. It features 14 EEG channels plus 2 references offering optimal positioning for accurate spatial resolution as shown in Figure 4. The software comes with EPOC can measure raw EEG data from the EPOC headset. Furthermore, through the software toolkit, the human's emotional states, facial expressions and mental commands can be captured by EPOC. The EPOC needs a training procedure to recognize what kind of thought pattern equates to a certain action as the same as OCZ NIA. The Emotiv software allows users to train the various thoughts

such as "pull", "stand up", "left", “right”, etc. It allows users to view their emotional state on a computational graph. It also provides a 2D blue avatar that allows the user to view their own facial expressions, and adjust the sensitivity of those detections. (Zhang, Wang, and Fuhlbrigge 2010, 379-384) The Emotiv EPOC and EPOC+ are sell for $399 and $499 USD, respectively.

Figure 4. The Emotive EPOC.

NeuroSky MindWave

NeuroSky MindWave headset takes decades of laboratory brainwave technology. It can safely measures brainwave signals and monitors the attention levels and meditation levels through the electrode placed on the forehead. More details about NeuroSky MindWave is discussed in Chapter 3.

Commercial Gaze Tracker

There are also some gaze-tracking products in the world. The most significant gaze-tracking product is Tobii Glasses. The Tobii glasses is design as a lightweight wearable eye tracking head unit. Through Tobii glasses, researchers are able to capture truly objective and deep insights into human behavior in any real-world environment. Tobii has developed their own eye tracking glasses for two generations. The newest generation called "Tobii Glasses 2" is upgrade to real-time tracking. Researchers can watch what a person's looking at on a tablet or laptop and the footage transmitted wirelessly from the glasses in real-time. The Tobii Glasses 2 consists of one high definition scene camera, four eye cameras, IR illuminators, gyroscope and accelerometer shown in Figure 5. Now Tobii Glasses 2 has been used in several areas, such as scientific research, market research, etc. The Tobii Glasses 2 sell with three different package. The price starts at $14,900 USD.

Figure 5. Tobii Glasses 2.

Open Source Gaze Trackers

Since the high performance commercial gaze trackers are expensive, building a gaze tracker by the researchers themselves becomes more popular. There are some self-build gaze tracker in the world. The most significant one seems to be the "openEyes" gaze tracker from Iowa State University. (Li, Babcock, and Parkhurst 2006, 95-100) The openEyes system consists of an open-hardware design which built from low-cost off-the-shelf components, and open-source software tools for eye-gaze tracking techniques. Both infrared and visible spectrum eye-tracking algorithms were developed and used to capture digital images, manipulate, and estimate the gaze direction. Moreover, the openEyes provides two types of eye-gaze tracking systems, head-mounted and remote eye trackers.

There are some other gaze trackers also worth to mention such as “Eye tracking off-the-shelf” from IT University Copenhagen (Hansen and others 2004, 58-58) or the “opengazer” from the Machine Intelligence Laboratory in Cambridge University Engineering Department. (Zielinski 2007)

.

CHAPTER II

THE HYBIRD BRAIN-COMPUTER INTERFACE

BCI systems are now used in various areas. However, different BCIs have their own advantages and disadvantages. In order to improve the performance of BCIs, Dr. Pfurtscheller et al proposed the hybrid BCI system which increasing advantages and reducing disadvantages from different BCIs. A hybrid BCI system is composed of two different BCIs, or at least one BCI and another system. A hybrid BCI must fulfill the following four criteria like any BCI: (i) the device must rely on signals recorded directly from the brain; (ii) there must be at least one recordable brain signal that the user can intentionally modulate to effect goal-directed behavior; (iii) real time processing; and (iv) the user must obtain feedback. (Pfurtscheller and others 2010) A hybrid BCI can either processing different inputs simultaneously, sequentially or in parallel. Figure 6 shows some examples of hybrid BCIs.

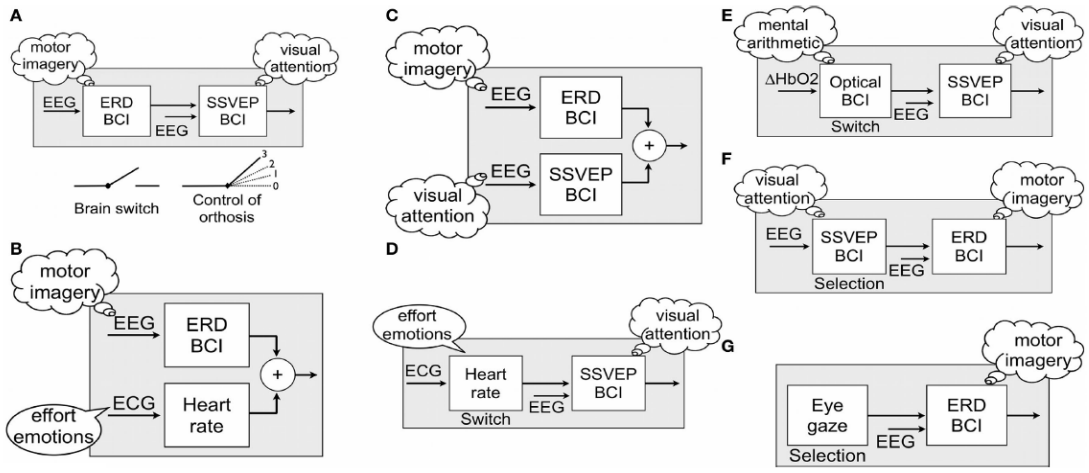

Figure 6. Examples of hybrid BCIs. (Pfurtscheller and others 2010)

In this thesis, a hybrid BCI system will be developed. The hybrid BCI consists of two different type of BCIs: Eye-Gaze Tracking and Electroencephalography (EEG). Both eye-gaze tracking and EEG will be introduced below.

Eye-gaze Tracking Technique

Only more recently, has the potential integration of eye movements in BCIs been seriously investigated. Lots of researches indicate the potential of eye-gaze tracking to enhance the quality of different BCIs. Human eyes can tell lots of things. Human's intention can be observed by eyes. Every person has the ability to control his or her own eyes and use them for output. Therefore, detection of eye gaze makes possible to extract human's intention which can be used in human and computer interaction. Nowadays, human eye is the best tool to communicate with computers except human hand.

Gaze tracking technologies have progressively become more accurate, efficient and less cumbersome. There are three major gaze tracking methods to track the motion of the eyes: electrooculography (EOG), searching coil in scleral contact lens and video-based eye tracking method. (Morimoto and Mimica 2005, 4-24)

Electrooculography (EOG)

Electrooculography (EOG) is a technique used as a diagnostic tool for studying the human oculomoter system. (Malmivuo and Plonsey 1995; Chen and Newman 2004, 243-248) The basic principle of EOG is to measure electric biopotentials exists between the front and the back of the human eye. It usually places two pairs of electrodes left and

right, above and below of the eye to measure eye movement and rotation as shown in Figure 7. The electric field of the eye is an electric dipole. When the eyeball move from left to right, the electric biopotential of right electrode become positive with respect to the left electrode. Regardless this method is sensitive to electro-magnetic interferences, it still works well already exists for a long time. Furthermore, it can measure the eye movement even when the eye is closed.

Figure 7. Electrodes of EOG placed around the eyes. (http://www.qubitbiology.com)

Searching Coil in Scleral Contact Lens

The technique of searching coil in scleral contact lens consists of a detection of the eye rotation by exploiting electromagnetic induction in a search coil embedded into a flexible contact lens as shown in Figure 8. (Carpi and Rossi 2009, 3-21) In particular, the user's gaze is detected by measuring the voltage induced in the search coil by an electromagnetic field generated externally. In fact, the direction and angular displacement of the eye change the polarity and amplitude of the induced voltage just

like EOG. Generally, a couple of external electromagnetic sources, arranged along orthogonal directions, can be used. Although very intrusive, search coil-based systems typically have a very high accuracy, about 0.08°. (Morimoto and Mimica 2005, 4-24) Latest developments of this technology include the useful development of wireless devices, so as to avoid the limitations typically introduced by the presence of the wire.

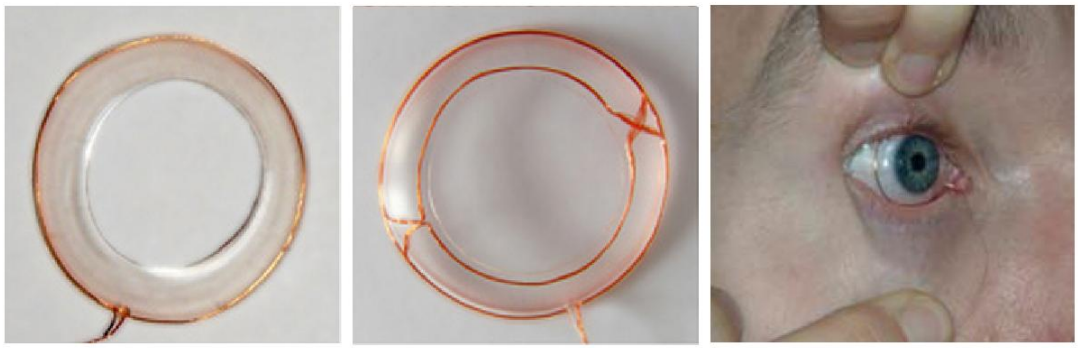

Figure 8. Scleral search coils contact lens. (http://www.chronos-vision.de)

Video-based Eye-gaze Tracking Technique

This method use a video camera connected to a computer for real-time image processing. The image processing is to detects the eye the pupil location and estimate the gaze direction through a mapping procedure. The significant advantage of video-based eye tracking is the unobtrusiveness.

The limbus and the pupil are common features used for tracking. (Morimoto and Mimica 2005, 4-24) Limbus is the boundary between the sclera and the iris. The human eye structure and appearance are shown in Figure 9 and 10. It can be easily tracked horizontally because of the contrast of these two regions. However, the limbus tracking

techniques are not widely used because eyelids will cover part of the iris. The reason above cause this techniques have low vertical accuracy. Compare to the limbus, the pupils are hard to detect and track because of the lower contrast. In order to enhance the contrast between the pupil and the iris, infrared (IR) illumination is developed. Researchers use an infrared light source to illuminate the pupil so the contrast between pupil and iris become significant. IR is a perfect tool to solve this task because IR is almost invisible for the human eye, but can still be captured by the video cameras. Most applications use near IR light sources with wavelength around 850 nm.

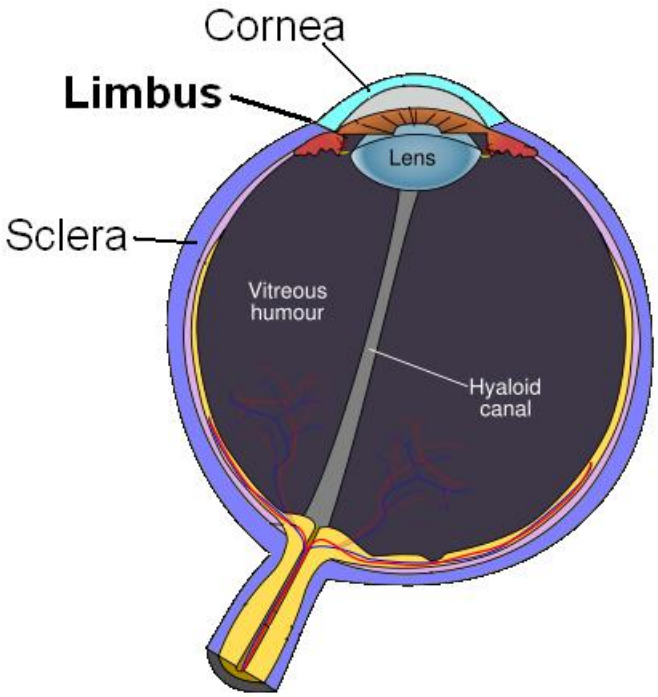

Figure 9. Human eye structure.

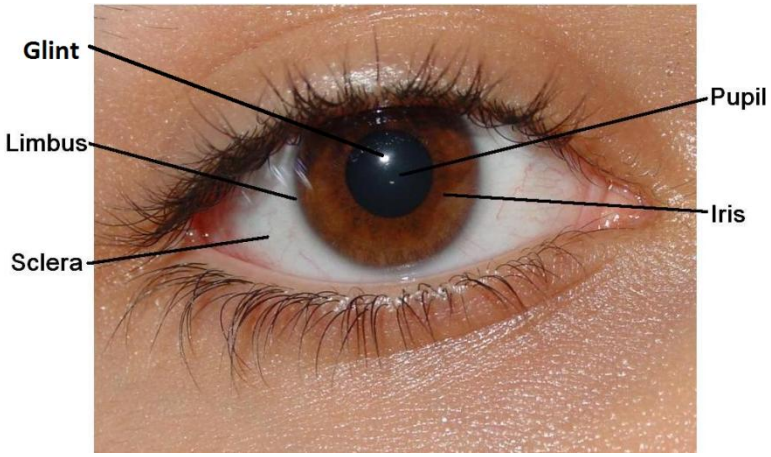

Figure 10. Human eye appearance.

The IR source also generates a corneal reflection or glint on the cornea surface near the pupil. This glint is used as a reference point in the pupil. Many video-based eye-gaze tracker are based on the corneal reflection method. (Morimoto and others 2000, 331-335) Generally, the eye-gaze tracker has a video camera with an IR LED mounted to illuminate the eye. After illuminating by the IR LED, a corneal reflection or glint will be appeared on the retina. Because the illumination has the same direction as the optical axis of the camera, the corneal reflection or glint location on the eye image stays in the same independent of gaze direction. The corneal reflection (glint) is shown in Figure 10.

The image processing software detects the position of the glint and the center of the pupil. The vector from the glint to the center of the pupil is the basis for the calculation of the gaze direction and finally the position of the gaze on the screen. A direct calculation would not only need the spatial geometry of the eye-gaze tracker, the IR LED, the display and the eye but also the radius of the eyeball, which is specific to the subject using the eye-gaze tracker. For this reason, a calibration procedure estimates

the parameters for the mapping of the glint-pupil vector to positions on the screen. (Drewes 2010) The aim of calibration is to map the location of pupil center respect to the screen to estimate the gaze point on the screen. More details of calibration procedure are introduced in Chapter 4.

Video-based Eye-gaze Tracking Algorithm

The corneal reflection or glint can be found in the last part. Then the location of pupil center becomes the next thing need to know. The objective of eye-tracking algorithm is to locate the pupil center. Eye-tracking algorithms can be classified into two approaches: feature-based and model-based approaches. (Li 2006) Feature-based approaches detect and localize image features related to the position of the eye. A commonality among feature-based approaches is that a criteria is needed to decide when a feature is present or absent. The determination of an appropriate threshold is typically left as a free parameter that is adjusted by the use. The tracked features vary widely across algorithms but most often rely on intensity levels or intensity gradients. For example, IR imagery the dual-threshold technique, an appropriately set intensity threshold can be used to extract the region corresponding to the pupil. The pupil center can be taken as the geometric center of this identified region. The intensity gradient can also be used to detect the pupil contour in infrared spectrum images or the limbus in visible spectrum images. Least-square fitting or circular though transform can then be used to fit an ellipse or a circle to these feature points. However, since feature point detection may be affected by eyelashes and eyelids, some additional process is needed to

eliminate false feature points. Pupil feature points are detected along radial vectors, but a method of rejecting outlines is not given. Feature points are delimited in a quadrilateral formed by the eye corners, the uppermost point of the upper eyelid and the lowermost of the lower eyelid. A double ellipse fitting approach is used as well. First, roughly detected feature points are used for ellipse fitting. And then feature points are detected again using the center of first ellipse as starting point. Finally, an ellipse is fitted to the feature points that are close enough to the first ellipse. A curvature function is applied to eliminate the artifacts of pupil edge. However, these methods may not be robust enough to a relatively large number of outliers and may not be able to remove all the outliers. On the other hand, model-based approaches do not explicitly detect features but rather find the best fitting model that is consistent with the image. For example, integral-differential operators can be used to find the best-fitting circle or ellipse for the limbus and pupil contour. This approach requires an iterative search of the model parameter space that maximizes the integral of the derivative along the contour of the circle or ellipse. (Li 2006)

The model-based approach can provide a more precise estimate of the pupil center than a feature-based approach given that a feature criteria is not applied to the image data. However, this approach requires searching a complex parameter space that can be fraught with local minima. Thus gradient techniques cannot be used without a good initial guess for the model parameters. Thus, the gain in accuracy of a model-based approach is obtained at a significant cost in terms of computational speed and flexibility.

Notably, the use of multi-scale image processing methods in combination with a model-based approach hold promise for real-time performance. (Li 2006)

Electroencephalography (EEG)

An electroencephalograph (EEG) is the recorded electrical activity generated by the brain. In general, EEG is obtained using electrodes placed on the scalp with a conductive gel. In the brain, there are millions of neurons, each of which generates small electric voltage fluctuations. The aggregate of these electric voltage fields create an electrical reading which electrodes on the scalp are able detect and record. Therefore, EEG is the superposition of many simpler signals. The amplitude of an EEG signal typically ranges from about 1μV to 100μV in a normal adult, and it is approximately 10 to 20 mV when measured with subdural electrodes such as needle electrodes. (Nicolas-Alonso and Gomez-Gil 2012, 1211-1279)

The EEG along the scalp usually measures in the range of 10μV-100μV and is band-limited in the frequency range 1Hz to 30Hz. Electrical activity recorded from ECoG and is usually measured in mV range. The human EEG was first recorded by German neurologist Hans Berger in 1924. To measure the EEG the standard international 10-20 system is used for placing scalp electrodes. (Malmivuo and Plonsey 1995; Bi, Fan, and Liu 2013, 161-176) The standard international 10-20 system is shown in Figure 11.

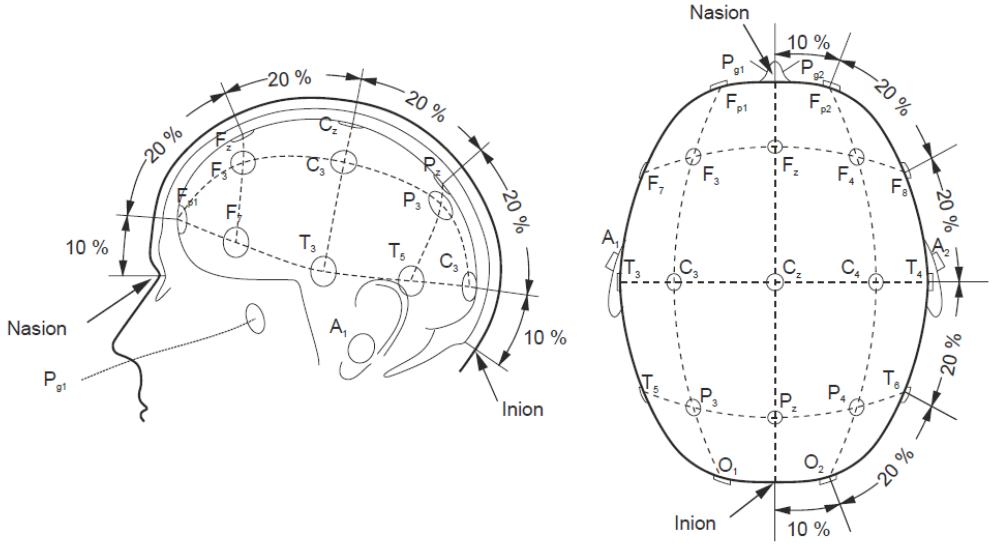

Figure 11. International 10-20 system.

The International 10–20 system is an internationally recognized method to describe and apply the location of scalp electrodes in the context of an EEG experiment. This method was developed to ensure standardized reproducibility so that a subject's studies could be compared over time and subjects could be compared to each other. This system is based on the relationship between the location of an electrode and the underlying area of cerebral cortex. The "10" and "20" refer to the fact that the actual distances between adjacent electrodes are either 10% or 20% of the total front–back or right–left distance of the skull.

Each site has a letter to identify the lobe and a number to identify the hemisphere location. The letters F, T, C, P and O stand for frontal, temporal, central, parietal, and occipital lobes, respectively. Note that there exists no central lobe; the "C" letter is used only for identification purposes. A "z" (zero) refers to an electrode placed on the

midline. Even numbers (2,4,6,8) refer to electrode positions on the right hemisphere, whereas odd numbers (1,3,5,7) refer to those on the left hemisphere. In addition, the letter codes A, P_g and F_p identify the earlobes, nasopharyngeal and frontal polar sites respectively.

EEG comprises a set of signals which may be classified according to their frequency. Some well-known frequency ranges have been defined according to distribution over the scalp. These frequency bands are referred to as delta, theta, alpha, beta, and gamma from low to high, respectively. Relevant characteristics of these bands are detailed below.

The delta band lies below 4 Hz, and the amplitude of delta signals detected in babies decreases as they age. Delta rhythms are usually only observed in adults in deep sleep state and are unusual in adults in an awake state. A large amount of delta activity in awake adults is abnormal and is related to neurological diseases. (Kübler and others 2001, 358) Due to low frequency, it is easy to confuse delta waves with artifact signals, which are caused by the large muscles of the neck or jaw. (Nicolas-Alonso and Gomez-Gil 2012, 1211-1279)

Theta waves lie within the 4 to 7 Hz range. In a normal awake adult, only a small amount of theta frequencies can be recorded. A larger amount of theta frequencies can be seen in young children, older children, and adults in drowsy, meditative or sleep states. Similar to delta waves, a large amount of theta activity in awake adults is related to neurological disease. (Kübler and others 2001, 358) Theta band has been associated

with meditative concentration. (Aftanas and Golocheikine 2001, 57-60; Nicolas-Alonso and Gomez-Gil 2012, 1211-1279)

Alpha rhythms are found over the occipital region in the brain. (Pineda 2005, 57-68) These waves lie within the 8 to 12 Hz range. Their amplitude increases when the eyes close and the body relaxes and they attenuate when the eyes open and mental effort is made. These rhythms primarily reflect visual processing in the occipital brain region and may also be related to the memory brain function. There is also evidence that alpha activity may be associated with mental effort. Increasing mental effort causes a suppression of alpha activity, particularly from the frontal areas. Consequently, these rhythms might be useful signals to measure mental effort. Mu rhythms may be found in the same range as alpha rhythms, although there are important physiological differences between both. In contrast to alpha rhythms, mu rhythms are strongly connected to motor activities and, in some cases, appear to correlate with beta rhythms. (Pineda 2005, 57-68; Nicolas-Alonso and Gomez-Gil 2012, 1211-1279)

Beta rhythms, within the 12 to 30 Hz range, are recorded in the frontal and central regions of the brain and are associated with motor activities. Beta rhythms are desynchronized during real movement or motor imagery. (Pfurtscheller and Neuper 2001, 1123-1134) Beta waves are characterized by their symmetrical distribution when there is no motor activity. However, in case of active movement, the beta waves attenuate, and their symmetrical distribution changes. (Nicolas-Alonso and Gomez-Gil 2012, 1211-1279)

Gamma rhythms belong to the frequency range from 30 to 100 Hz. The presence of gamma waves in the brain activity of a healthy adult is related to certain motor functions or perceptions. (Lee and others 2003, 57-78) Some experiments have revealed a relationship in normal humans between motor activities and gamma waves during maximal muscle contraction. This gamma band coherence is replaced by a beta band coherence during weak contractions, suggesting a correlation between gamma or beta cortical oscillatory activity and force. Also, several studies have provided evidence for the role of gamma activity in the perception of both visual and auditory stimuli. Gamma rhythms are less commonly used in EEG-based BCI systems, because artifacts such as electromyography (EMG) or electrooculography (EOG) are likely to affect them. (Zhang and others 2010, 51-60) Nevertheless, this range is attracting growing attention in BCI research because, compared to traditional beta and alpha signals, gamma activity may increase the information transfer rate and offer higher spatial specifity. (Nicolas-Alonso and Gomez-Gil 2012, 1211-1279) Table 2 shows the characteristics of some types of brainwave classified by frequency bands.

Brainwave type	**Frequency range**	**Mental states and condition**
Delta	1 – 4Hz	Deep, dreamless sleep, unconscious
Theta	4 – 7 Hz	Drowsiness or arousal in older children and adults

Table 2. The characteristics of different brainwave type

Brainwave type	Frequency range	Mental states and condition
Alpha	7 – 12 Hz	Relaxed, closing eyes, but not drowsy
Beta	12 – 30 Hz	Active, busy, or anxious thinking, active concentration, alertness
Gamma	30 – 100+ Hz	Higher mental activity, tactile sensations

Table 2. Continued

The Proposed Hybrid BCI System

The main obstacle to integrating eye-gaze tracking techniques into brain computer interfaces is that they have been either high risk or expensive for routine use. Current commercial eye-gaze trackers are expensive(over $10,000 USD) due to high accuracy and well-looking appearance. The cost of these commercial eye-gaze tracker contains not only the high-quality digital camera and the well-looking appearance, but also custom software implementation which can obtain high accuracy and fast performance. Furthermore, some BCIs are high risk or require special equipments such as special contact lenses, fMRI machine, electrodes, etc.

In order to eliminate the disadvantages above, a low cost hybrid BCI system combines with gaze tracking and EEG techniques is developed in this thesis. The hybrid BCI system is designed as a light-weight, head-mounted device, so that both the eye-gaze tracking direction and brainwave can be acquired by wearing only one device that

includes one sensing node, an eye camera and a scene camera. A self-build eye-gaze tracker with two cameras will be introduced in the next two chapters and it only cost less than $100 USD. The eye-gaze tracking algorithm is developed and programmed in LabVIEW.

Moreover, NeuroSky MindWave is used for EEG acquisition. When the NeuroSky MindWave is worn, one electrode will be placed at "F_{p1}" based on the International 10-20 system. The location "F_{p1}" is the most effective locations to determine concentration and meditation. (Kubota and others 2001, 281-287) Besides, eye blinking can be detected by EOG in the same location. The NeuroSky MindWave is sold for $79.99 USD on the market. So the total cost of the hybrid BCI system cost about $150 USD. It is much cheaper than the commercial eye-gaze trackers and medical EEG equipments mentioned above. Furthermore, it can achieve 80% performance of commercial eye-gaze trackers and medical EEG equipments and the cost is just 2% of them.

CHAPTER III

HARDWARE DESIGN

In this thesis, a self-build eye-gaze tracker and a commercial EEG product will be used. The cost of the eye-gaze tracker includes two cameras and NeuroSky MindWave are $58.43 USD and $79.99 USD respectively. The total cost of the hardware in this thesis is $138.42 USD. The design of the eye-gaze tracker and NeuroSky MindWave is depicted below.

Self-build Eye-gaze Tracker

The eye-gaze tracker is designed for head mounted and mobile use. It works in infrared spectrum using dark pupil effects. The eye-gaze tracker consists of one camera for eye tracking, one camera for scene viewing, three IR LED, one 22 ohm resistor, an IR pass filter and a glasses frame. The construction of the eye-gaze tracker is based on (Mantiuk and others 2012; Babcock, Pelz, and Peak 2003; Li, Babcock, and Parkhurst 2006, 95-100; Abbott and Faisal 2012, 046016) The materials are listed in Table 3.

The glasses are made of off-the-shelf component. The main part of glasses is the eye capture module shown as Figure 12A. It is responsible for providing an image of the eye to the computer. The main part of the module is the circuit inside Microsoft LifeCam VX-1000 webcam. The Microsoft VX-1000 webcam is disassembled and only the circuit with camera lens is used. Then we remove the IR filter in the original camera lens and put a piece of exposed negative film to replace the IR filter. The exposed negative

film can be treated as an IR pass filter that allows capturing images in IR light which is shown in Figure 12A-B. The eye capture module can connect to a computer via USB port. Based on the USB technical specification an IR illumination system was integrated with the eye capture module. Three IR LEDs are placed on the capture module and supplied by USB cable the same as the lens shown as in Figure 12C. This solution is very practical. The eye capture module is placed at the end of the an aluminum wire and then mounted to the modified a glasses frame. In the end, the scene camera is placed on the sensor arm of NeuroSky Mindwave. The complete self-build eye-gaze tracker is shown in Figure 16.

Part name	**Quantity**	**Cost**
Microsoft LifeCam webcam VX-1000 (for eye tracking)	1	$20
Microsoft LifeCam webcam NX-3000 (for scene)	1	$20
Safety glasses frame	1	$5.95
IR LED	3	$3.76
Carbon resistor 1/4W 22R	1	$0.78
Exposed negative film	20 cm	$4.95
Aluminum wire ø 5mm	30 cm	$1
Mounting strips 2.4mm x 100mm	3	$0.99
Heat shrinkable tubin ø 10mm	10 cm	$1
		Total: $58.43

Table 3. Materials of self-build gaze tracker

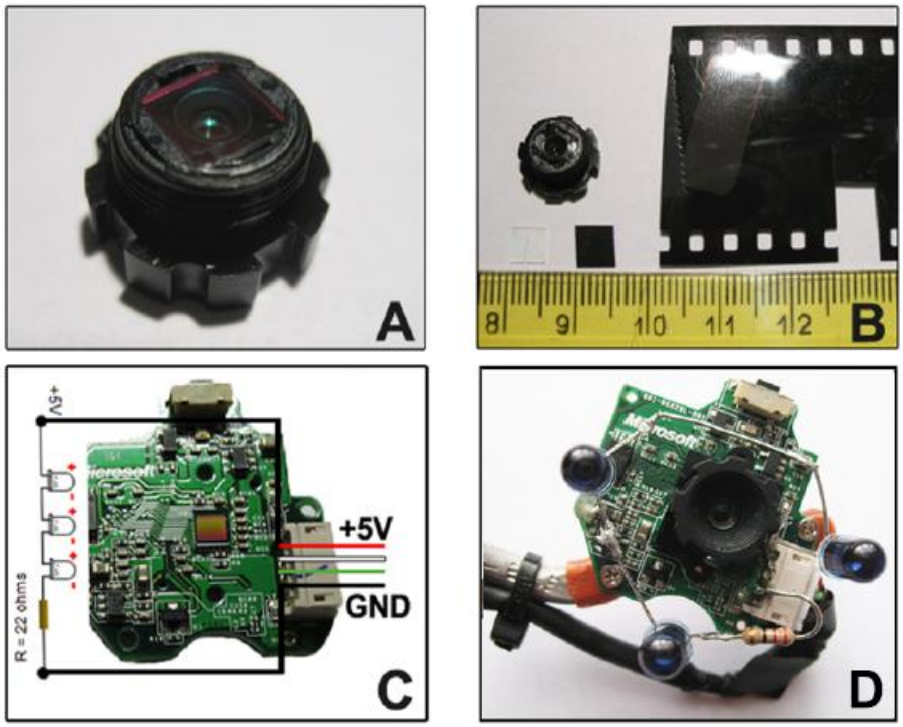

Figure 12. The construction of eye capture module. (A) Original lens of Microsoft VX-1000 with IR filter. (B) IR pass filter (exposed negative film). (C) IR LEDs mounted on the circuit. (D) Complete eye capture module.

The eye capture module is equipped with IR LEDs to additionally illuminate the eye in the infrared spectrum. Positions of IR LEDs are carefully chosen to assure correct illumination of the eye and avoid strong corneal reflection which could affect results of the pupil detection algorithm. Figure 13 shows the difference between image taken with different filters. (Mantiuk and others 2012) Here three IR LEDs with 850nm wavelength spread in the triangle topology around the camera lens give satisfactory results.

Figure 13. Image captured by a webcam. (A) With IR filter only. (B) With IR pass filter only. (C) With IR pass filter and illuminate by IR LED. (Mantiuk and others 2012)

NeuroSky MindWave

The NeuruSky MindWave is a single-channel EEG device produced by Neurosky Inc. The NeuroSky MindWave consists of eight main parts, ear clip, flexible ear arm, battery area, power switch, adjustable head band, sensor tip, sensor arm and inside ThinkGear chipset. This device use a dry sensor to measure the EEG signals from the forehead. The sensor tip is placed at "F_{p1}" location based on the International 10-20 system. At the same time, the sensor pick up ambient noise generated by human muscle, computers, light bulbs, electrical sockets and other electrical devices. This headset contains NeuroSky ThinkGear technology which measures the analog electrical signals and processes them into digital signals. The ear clip is a grounds and reference which allows ThinkGear chip to filter out the electrical noise. Then the chip transmits the filtered data to a laptop/PC via bluetooth. (Salabun 2014, 169-174) The structure of MindWave headset is shown in Figure 14.

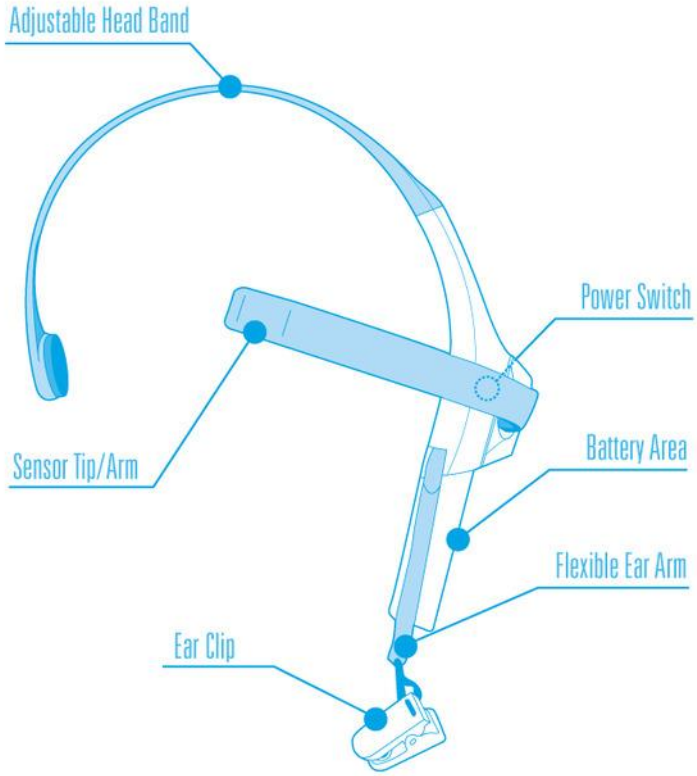

Figure 14. NeuroSky Mindwave headset.

NeuroSky Mindwave can measure raw EEG signals, power spectrum (alpha, beta, delta, gamma, theta), attention level, mediation level and eye blinking. The raw EEG data received at a rate of 512 Hz. Other measured values are made every second. Therefore, raw EEG data is a main source of information on EEG signals using MindWave.

On the producer webpage, more than 130 applications can be found which is classified into 4 platforms, 5 genres and 16 developers. These apps do not provide the source code. Therefore, change of functionality is not possible. However, dynamic-link library (thinkgear.dll) is available to handle the connection to the device. Moreover, we can develop our won applications through MATLAB or LabVIEW software. The

MATLAB and LavVIEW allow to include the thinkgear.dll so the researchers can utilize it for scientific researches. Figure 15 shows the communications protocol between MATLAB and MindWave headset.

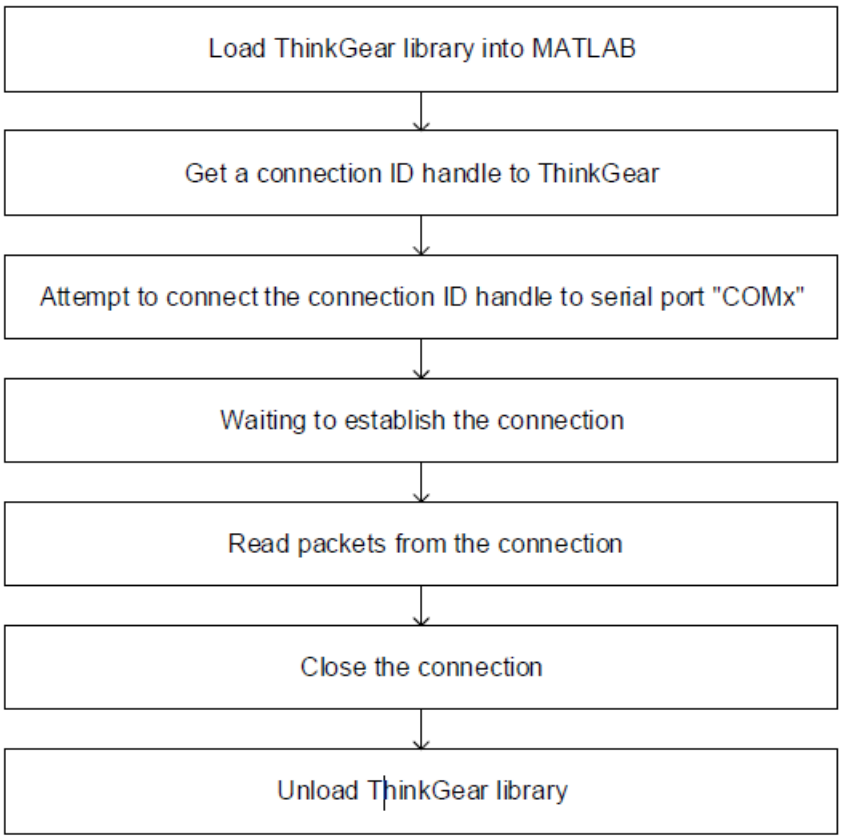

Figure 15. Communication protocol between MATLAB and MindWave. (Salabun 2014, 169-174)

At last, the eye-gaze tracker and NeuroSky MindWave headset can be integrated together as a hybrid BCI device combined with gaze tracking and EEG. The complete hybrid BCI hardware is shown in Figure 16.

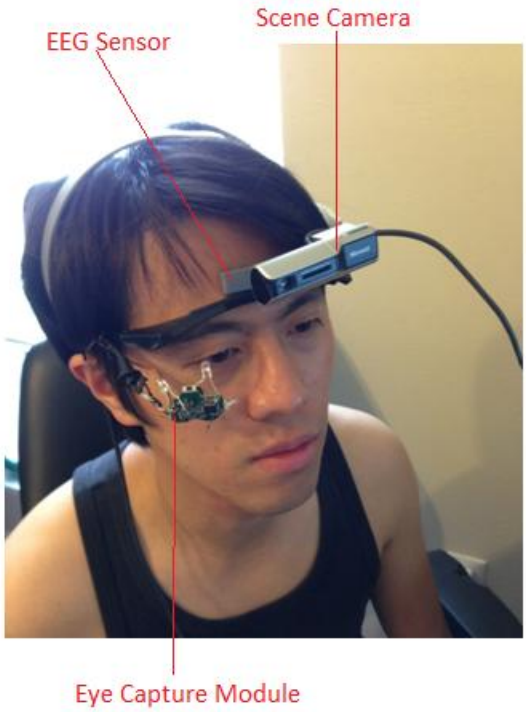

Figure 16. The hardware of proposed hybrid BCI system.

CHAPTER IV

SOFTWARE DESIGN

Presented in this chapter are two algorithms both developed in National Instrument LabVIEW: eye-gaze tracking algorithm and EEG algorithm. The eye-gaze tracking algorithm developed in the feature-based approach. The objective of this algorithm is to extract the location of the pupil center so as to map it to the scene image. The EEG algorithm is designed to detect human's attention level, meditation level and eye-blinking times. These two algorithms is introduced respectively below.

Eye-gaze Tracking Algorithm

The main goal of eye-gaze tracking algorithm is to locate the pupil center and project the estimated gaze direction onto the scene image. The eye-gaze tracking can be divided into two parts: eye feature detection and gaze estimation. Eye feature detection is to obtain the location of pupil center. Gaze estimation transforms the locations of pupil center to gaze direction in the scene image through a calibration procedure. A general eye-gaze tracking calibration procedure is shown in Figure 17.

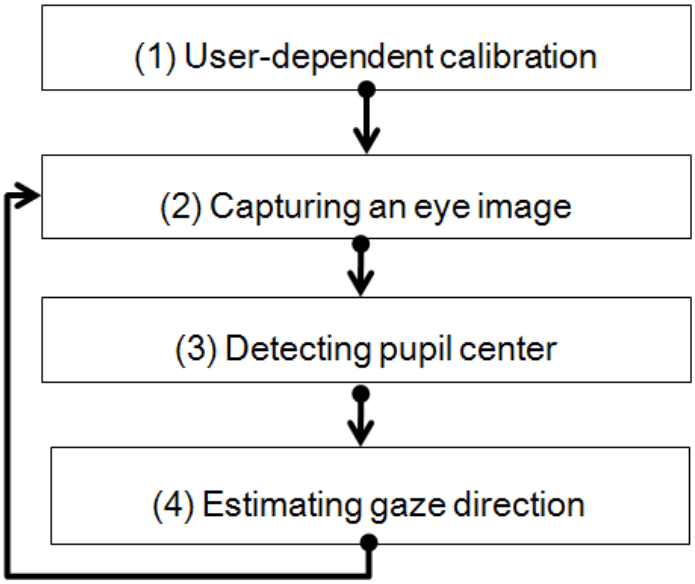

Figure 17. The flow chart of eye-gaze tracking algorithm.

Eye feature detection

The objective of eye feature detection is to locate the pupil center from the eye image. Designing the eye-tracking algorithm we took advantage of NI Vision Development module. First step of the image processing is using the IMAQ Local Threshold function, that applies an adaptive threshold to a binary image as shown in Figure 18B. This function requires a lot of processor time to be executed and the larger the image the more time it requires. So the resolution of image is set to 320x240 pixels.

The second step is to apply edge remove and fill hole function. Edge remove function helps to eliminate particles that touch the border of the eye image and fill hole function can fill the hole in the pupil particle which caused by the glints as shown in Figure 18C.

The third step is to apply a particle filter to distinguish the pupil from other dark particles and estimate its center of mass as shown in Figure 18D. Through the particle analysis report function, the pupil center can be found in the end shown as in Figure 18E.

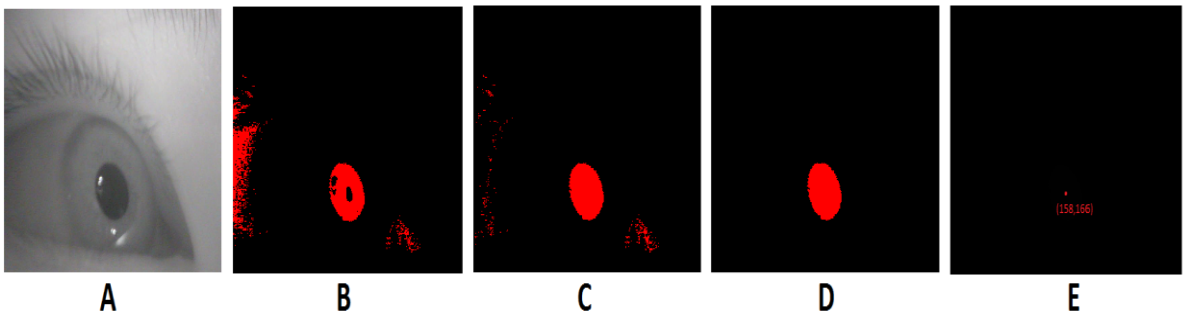

Figure 18. Eye feature detection procedure. (A) Original eye image. (B) Convert to a binary image by applying a threshold. (C) Apply edge remove and fill hole function. (D) Apply a particle filter. (E) The location of pupil center.

Calibration

In order to calculate the point of gaze in the scene image, a mapping must be constructed between eye-position coordinates and scene-image coordinates. The mapping can be initialized by relating known eye positions to known scene locations. The typical procedure in eye-tracking methodology is to measure this relationship through a calibration procedure. In this thesis, the user is required to look at nine points of scene image during calibration. Figure 19 shows the mappings between the pupil movable area defined by the nine pupil centers at calibration procedure and nine reference points in the scene image. (Lee, Heo, and Park 2013, 10802-10822)

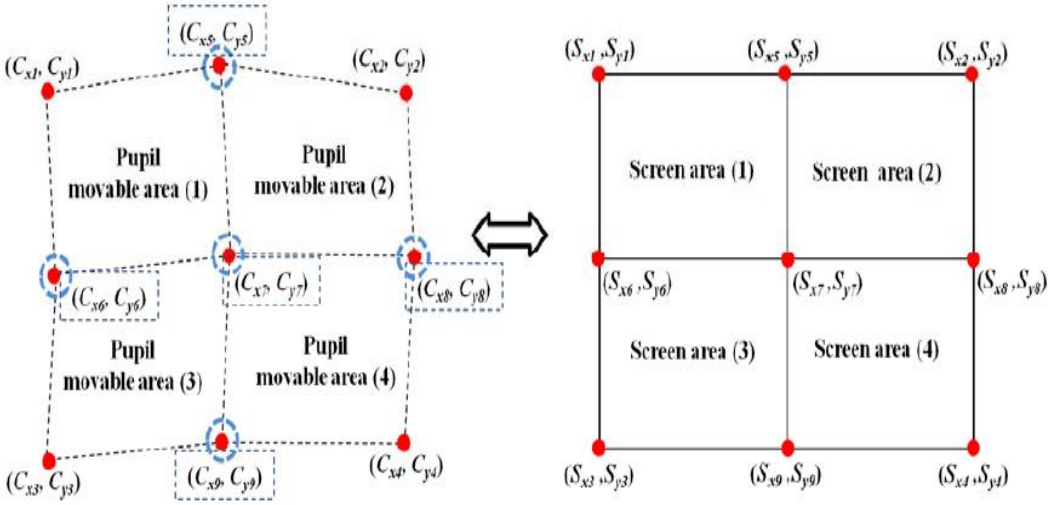

Figure 19. Pupil center locations mapping to reference points of scene image.

The pupil movable area constructed by nine pupil center locations can be divided into four areas as shown in Figure 19. Pupil movable area 1 maps to scene area1, pupil movable area 2 maps to scene area 2, and so on. For example, pupil movable area 1 is defined by (C_{x1}, C_{y1}), (C_{x5}, C_{y5}), (C_{x6}, C_{y6}), (C_{x7}, C_{y7}) which maps to scene area 1. And the mapping function is defined as a transform matrix T_1 between pupil movable area 1 and scene area 1 as shown in Figure 20 and 21.

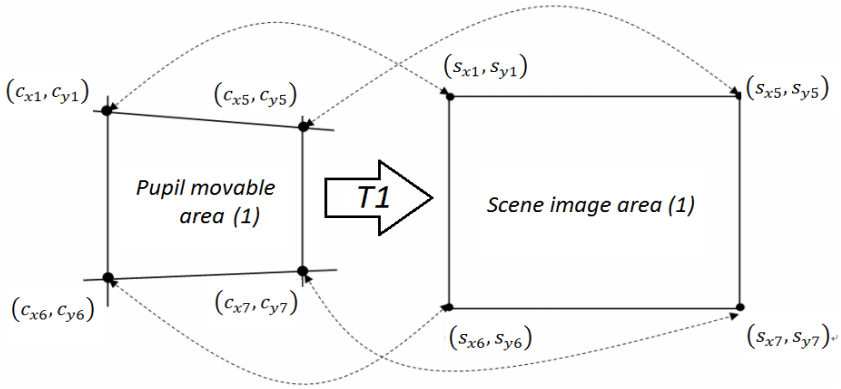

Figure 20. Mapping between pupil movable area 1 and scene image area 1.

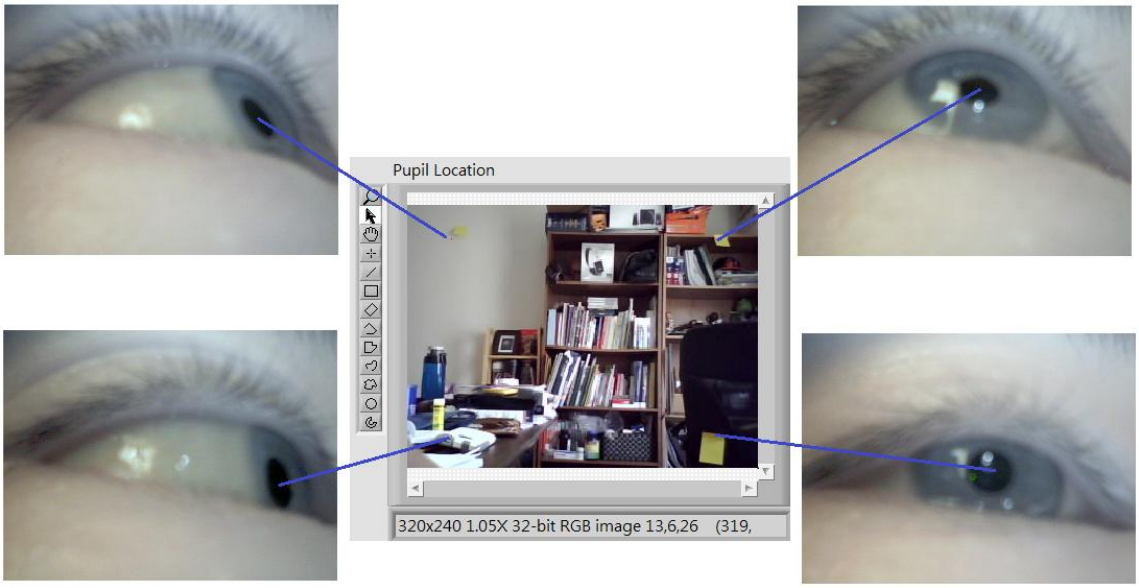

Figure 21. Four pupil center location respect to four reference point in scene image.

To determine the transform between the distorted quadrangle area and the rectangle area, a geometric transform method is used based on the following equations

(Gonzalez and Woods 2002; Cho and others 2009a, 127202-127202-15; Lee and others 2010, 289-298):

$$S_x = a \cdot C_x + b \cdot C_y + c \cdot C_x C_y + d, \tag{3.1}$$

$$S_y = e \cdot C_x + f \cdot C_y + g \cdot C_x C_y + h \tag{3.2}$$

Equations (3.1) and (3.2) are based on a bilinear approximation which commonly used in image registration. This geometric transform method can transform a distorted image into a normal image. As shown in Equation (3.1) and (3.2), the 1st-order polynomial function includes eight parameters which consider the 2D factor of rotation, translation, scaling, parallel inclining, and distortion between (C_x, C_y) and (S_x, S_y). (Lee, Heo, and Park 2013, 10802-10822) In order to obtain the value of eight unknown parameters, a transform matrix T is represented as follows:

$$S = T \ C$$

$$\begin{bmatrix} S_x \\ S_y \\ 0 \\ 0 \end{bmatrix} = \begin{bmatrix} a & b & c & d \\ e & f & g & h \\ 0 & 0 & 0 & 0 \\ 0 & 0 & 0 & 0 \end{bmatrix} \begin{bmatrix} C_x \\ C_y \\ C_x C_y \\ 1 \end{bmatrix} \tag{3.3}$$

In this thesis, multi-geometric transformations (multiple 1st-order polynomial functions) with the nine calibration points is used as shown in Figure 19. Four mapping transforms (T_1, T_2, T_3 and T_4) are defined between four pupil movable areas and four scene image areas, as shown in Figure 22.

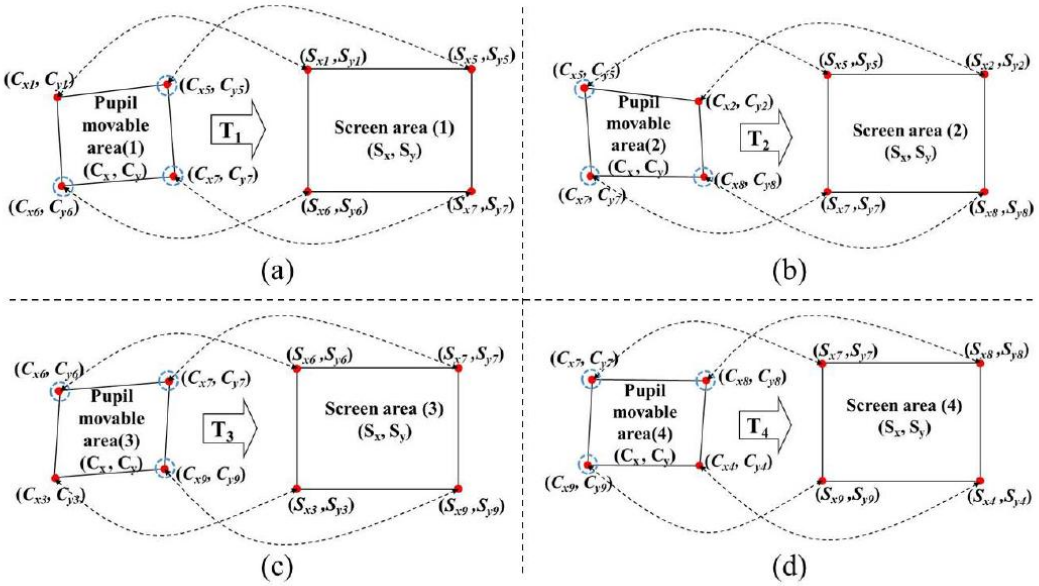

Figure 22. Mapping transforms. (A) Between pupil movable area 1 and scene image area 1. (B) Between pupil movable area 2 and scene image area 2. (C) Between pupil movable area 3 and scene image area 3. (D) Between pupil movable area 1 and scene image area 1.

As shown in Figure 22A, T_1 is the mapping transform matrix between pupil movable area 1 and scene area 1. Using the training data, the matrix T_1 can be obtained in advance by multiplying S_1 and the inverse matrix of C_1 in the equation below (Lee, Heo, and Park 2013, 10802-10822):

$$S_1 = T_1\, C_1$$

$$\begin{bmatrix} S_{x1} & S_{x5} & S_{x6} & S_{x7} \\ S_{y1} & S_{y5} & S_{y6} & S_{y7} \\ 0 & 0 & 0 & 0 \\ 0 & 0 & 0 & 0 \end{bmatrix} = \begin{bmatrix} a_1 & b_1 & c_1 & d_1 \\ e_1 & f_1 & g_1 & h_1 \\ 0 & 0 & 0 & 0 \\ 0 & 0 & 0 & 0 \end{bmatrix} \begin{bmatrix} C_{x1} & C_{x5} & C_{x6} & C_{x7} \\ C_{y1} & C_{y5} & C_{y6} & C_{y7} \\ C_{x1}C_{y1} & C_{x5}C_{y5} & C_{x6}C_{y6} & C_{x7}C_{y7} \\ 1 & 1 & 1 & 1 \end{bmatrix} \quad (3.4)$$

By applying the same calculation above, transform matrices T_2, T_3 and T_4 can be obtained via respective locations of pupil center. Then the gaze point can be estimated on the scene image via the equation below:

$$G = T\ C$$

$$\begin{bmatrix} G_x \\ G_y \\ 0 \\ 0 \end{bmatrix} = \begin{bmatrix} a & b & c & d \\ e & f & g & h \\ 0 & 0 & 0 & 0 \\ 0 & 0 & 0 & 0 \end{bmatrix} \begin{bmatrix} C_x \\ C_y \\ C_x C_y \\ 1 \end{bmatrix} \tag{3.5}$$

During the tracking stage, if the location of pupil center belongs to the quadrangle of pupil movable area 1, the T_1 matrix in Equation (3.4) is selected and the gaze point (G_x, G_y) on the scene image is calculated by multiplying T_1 and C. By the same method, the pupil center locates in pupil movable area 2, 3 or 4 can be calculated by multiplying T_2, T_3 or T_4 and C respectively.

Previous studies (Cho and others 2009b, 127202-127202-15; Lee and others 2010, 289-298) also used the 1st-order polynomial function (geometric transform) to map the pupil movable area onto the screen area. However, the main difference between the gaze-tracking method in this research and the previous methods is that multi-geometric transform matrices (T_1, T_2, T_3 and T_4) is used, whereas previous studies used only one single geometric transform matrix to map the quadrangle defined by (C_{x1}, C_{y1}), (C_{x2}, C_{y2}), (C_{x3}, C_{y3}) and (C_{x4}, C_{y4}) into the rectangle defined by (S_{x1}, S_{y1}), (S_{x2}, S_{y2}), (S_{x3}, S_{y3}) and (S_{x4}, S_{y4}). Compare with the method in previous studies, multi-geometric transform matrices method is more robust and accurate.

EEG Algorithm

Raw EEG data is essentially a summation of various brain wave oscillations and artifacts. It includes alpha, beta, theta, delta and gamma waves. The beta wave in particular can be attributed to the “attention” part of the brain activity and this is what is being used to control the output magnitude. In proportion to beta wave, alpha wave can be attributed to the "meditation" part of the brain activity.

NeuroSky Inc. provides the NeuroSky Driver for LabVIEW which allows users to easily acquire data and access the full functionality of the system level driver. NeuroSky provides a dynamic linked library (DLL) with a set of functions written in C that access the virtual com port that runs with the MindWave headset. Instead of accessing the specific DLL functions, LabVIEW users can now use the NeuroSky Driver for LabVIEW to easily access data from the NeuroSky driver in minutes. The NeuroSky Driver for LabVIEW includes specific band pass filters, attention and meditation level acquisition, eye blink detection, eye blink strength, etc. In order to determine the command of grasp or release, a EEG algorithm is developed shown in Table 4.

Commands Type		**Eye blinks times in 1.5 second period**	
		Double	*Triple*
Attention level	*Low*	Release	Arm withdraw
	High	Grasp	Arm reaching object
Meditation Level	*Low*	Grasp	Arm reaching object
	High	Release	Arm withdraw

Table 4. Proposed EEG algorithm to control prosthetic arm

The attention and meditation level can be observed at the same time shown in Figure 23. Two threshold is set in both attention and meditation to determine the levels is high or low. The high threshold value is set to 85 and the low threshold value is set to 20. For example, the attention level is high in the period 11s-12.5s, 22.1s-24.8s and 27s-28.5s and the meditation level is high in the period 69.9s-61.9s, 88.0s-91.5s and 95.2s-96.3s as shown in Figure 23.

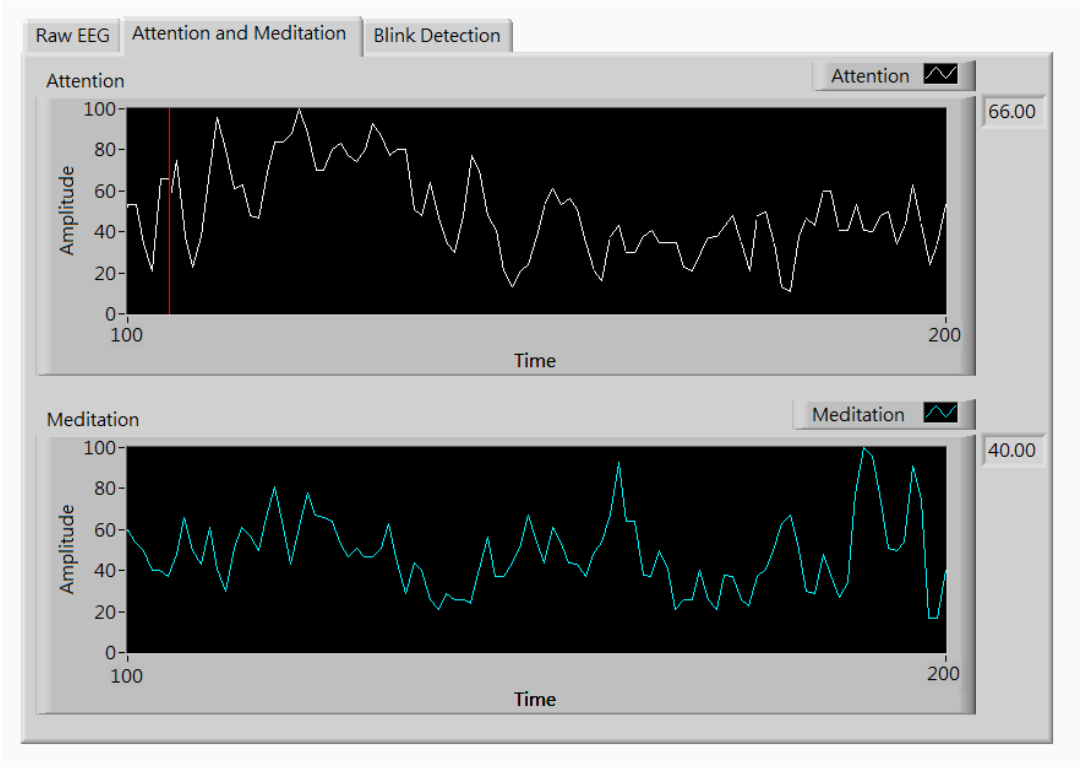

Figure 23. Attention level and meditation level.

The eye blink is relatively easy to observe from raw EEG signal. The amplitude of eye blink signal is more larger than the EEG signal shown in Figure 24. A threshold is set as well to determine there is eye blink or not.

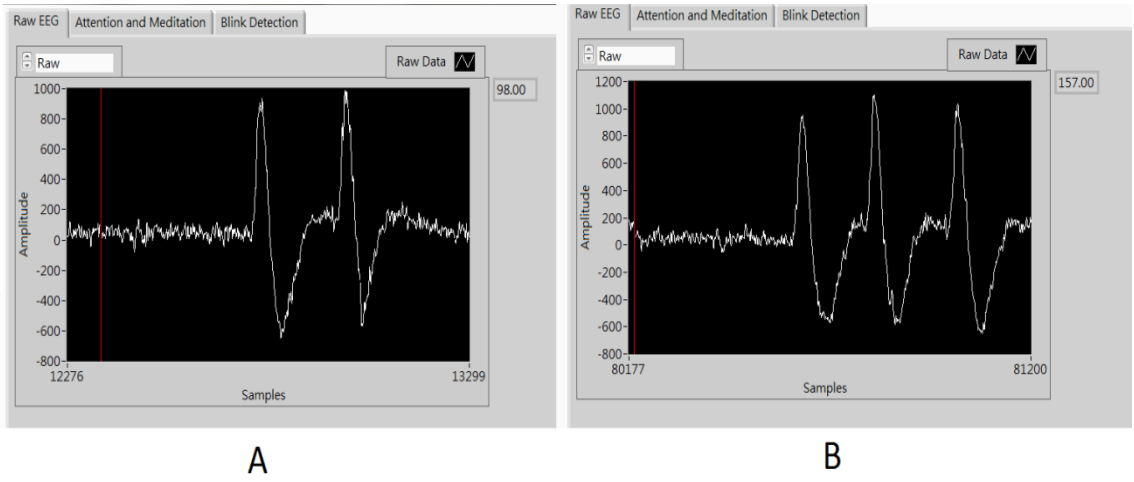

Figure 24. Eye blink signals. (A) Double eye blinks. (B) Triple eye blinks.

Proposed Hybrid Algorithm

Combining the eye-gaze tracking and EEG algorithm above, a hybrid BCI system is proposed in this thesis. Suppose a person want to grasp one subject in front of him/her, the location of this subject in the scene camera can be obtained via the eye-gaze tracker and grasp/release command can send via the EEG BCI. Figure 25 shows the overall procedure of the hybrid BCI.

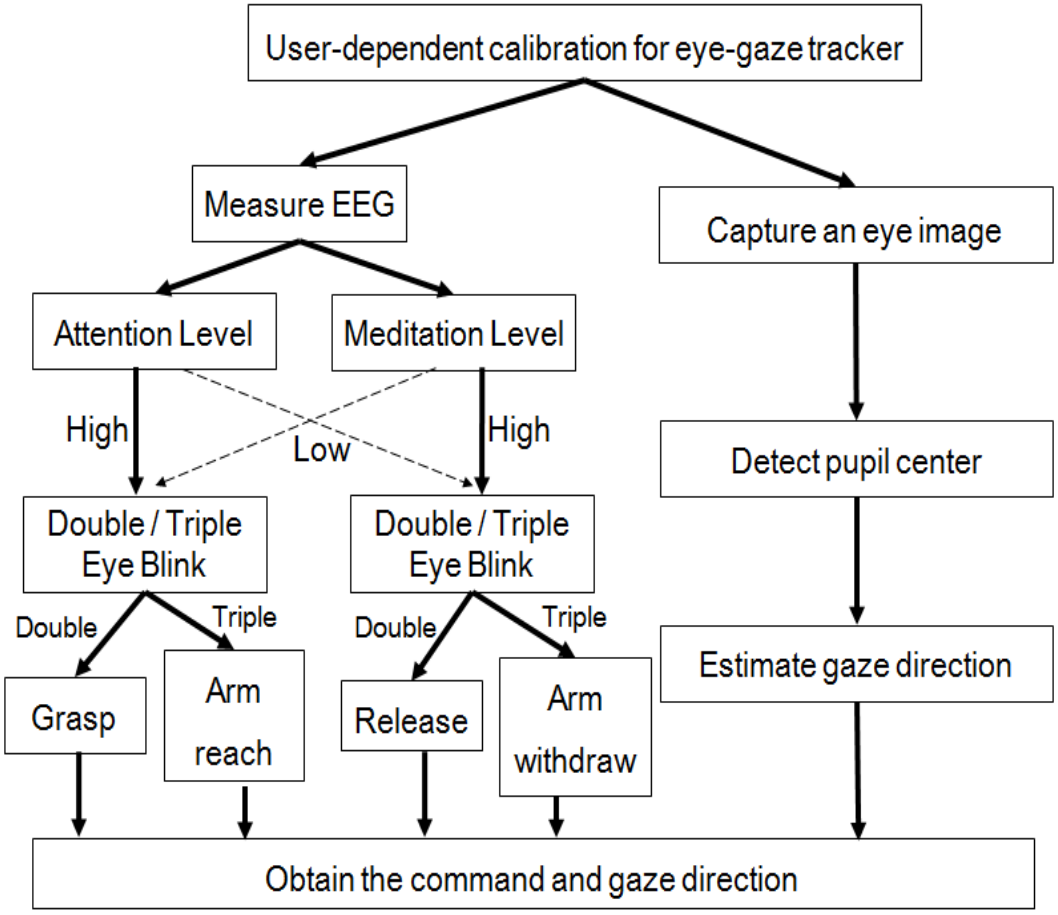

Figure 25. Overall procedure of proposed hybrid BCI system.

CHAPTER V

EXPERIMENTAL SETUP, RESULT AND CONCLUSION

This chapter will discuss the experimental setup and result for both eye-gaze tracker and NeuroSky Mindwave.

Experimental Setup

In the beginning, the user-dependent calibration is needed. After wearing the eye-gaze tracker and NeuroSky MindWave headset well, the calibration could be started. Nine point are chosen in the scene image as reference point. The coordinates of these reference points are: (5,5), (160,5), (315, 5), (5,120), (160,120), (315,120), (5,235), (160,235) and (315,235). After the calculation, four transform matrices T_1, T_2, T_3 and T_4 can be obtained. Then we input the values of T_1, T_2, T_3 and T_4 into the LabVIEW program to finish the user-dependent calibration.

Before using the NeuroSky MindWave headset, a training procedure is required. The training procedure helps the NeuroSky MindWave headset to accommodate to user's brain activity. The user can watch a short training video that helps the user accommodate to the headset quicker. (Nussbaum and Hargraves 2013) The training procedure usually takes 10 to 15 minutes. Once the calibration and training procedure are finished, the program can start to run and the user can start to use the hybrid BCI system. Figure 26 and 27 shows the GUI of eye-gaze tracking and EEG, respectively.

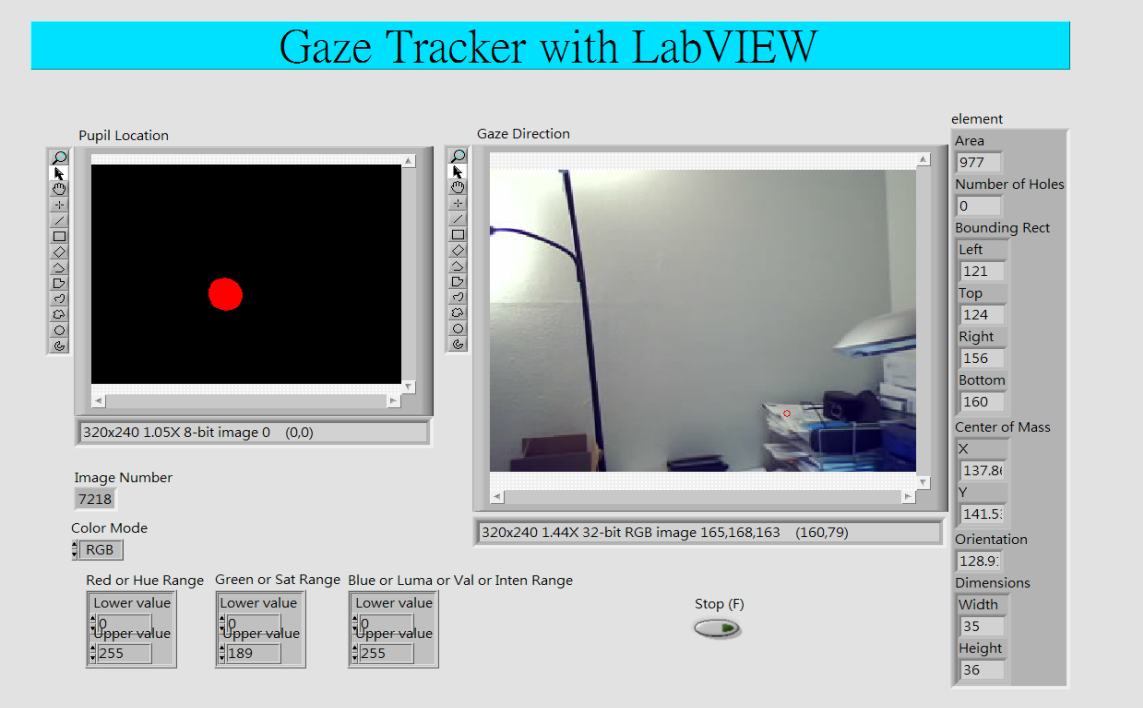

Figure 26. GUI of eye-gaze tracking.

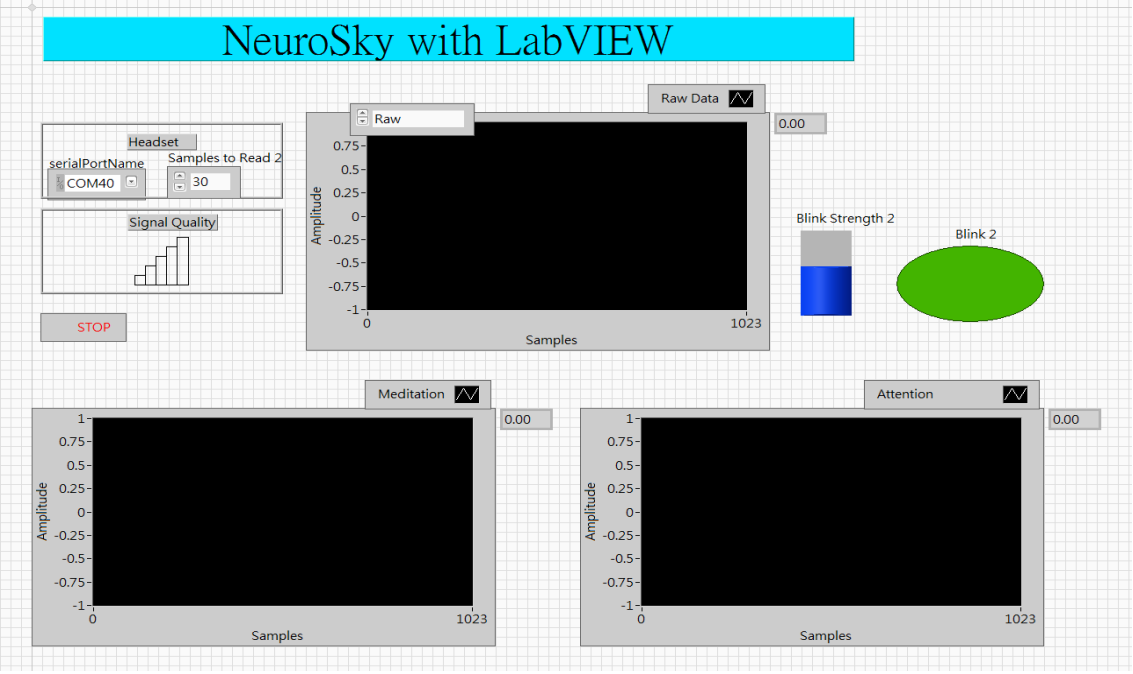

Figure 27. GUI of NeuroSky MindWave.

Experimental Result

The proposed hXybrid BCI was tested on a laptop with an Intel Core i5-2520M 2.50 GHz CPU and 8 GB RAM. All the algorithms is developed in LabVIEW. In the experiments, the user gazed at nine reference points in the scene which project by a laser pointer in each trial and the user have to finish four trials. The results shows in Figure 28.

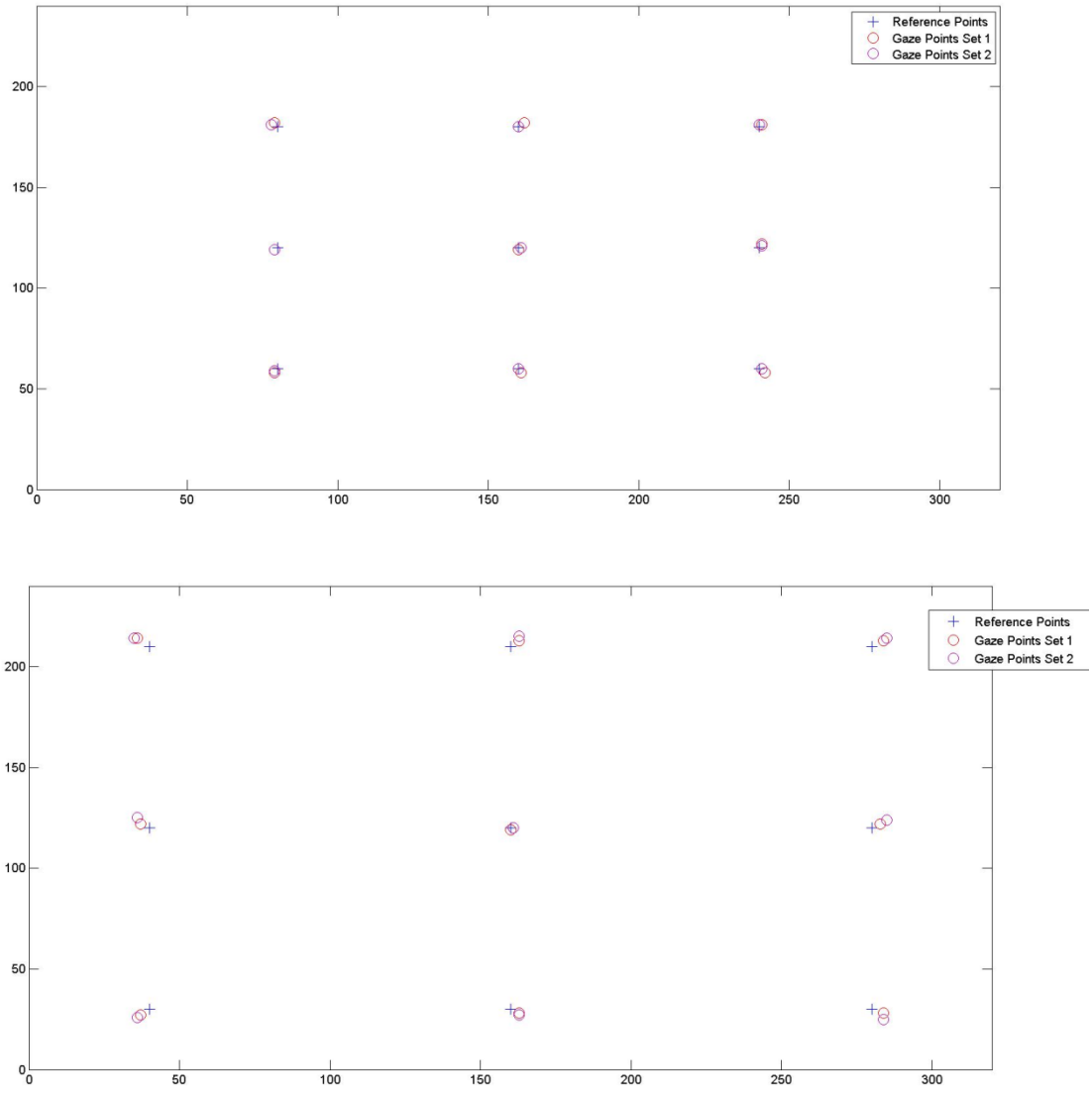

Figure 28. The estimate gaze points with respect to the reference points.

Conclusion

This thesis has demonstrated the development of a low-cost, light weight, high performance hybrid brain-computer interface combining eye-gaze tracking and EEG. By combining these two different BCIs, the human's intention can be captured without using any muscle. The eye-gaze tracker built with a scene camera can obtain the human gaze direction, and EEG BCI can measure human's attention and meditation. Based on the facts, some algorithms can be designed to control intelligent prostheses. The experimental result shows that the accuracy is good enough to estimate the gaze direction compared with the expensive commercial eye-gaze trackers. Furthermore, the cost of the hybrid BCI system is low enough for individual researchers.

In future work, some machine vision algorithms need to be developed in order to determine the distance between the user and desired reaching object. And error detect algorithm also needs to be built if the gaze point is not correct on the desired reaching object.

REFERENCES

Abbott, WW and AA Faisal. "Ultra-Low-Cost 3D Gaze Estimation: An Intuitive High Information Throughput Compliment to Direct Brain–machine Interfaces." *Journal of Neural Engineering* 9, no. 4 (2012): 046016.

Aftanas, LI and SA Golocheikine. "Human Anterior and Frontal Midline Theta and Lower Alpha Reflect Emotionally Positive State and Internalized Attention: High-Resolution EEG Investigation of Meditation." *Neuroscience Letters* 310, no. 1 (2001): 57-60.

Babcock, Jason, Jeff Pelz, and Joseph Peak. "The Wearable Eyetracker: A Tool for the Study of High-Level Visual Tasks." In *Proceedings of the Military Sensing Symposia Specialty Group on Camouflage, Concealment, and Deception,* Tucson, Arizona. (2003).

Bi, Luzheng, Xin-An Fan, and Yili Liu. "EEG-Based Brain-Controlled Mobile Robots: A Survey." *Human-Machine Systems, IEEE Transactions On* 43, no. 2 (2013): 161-176.

Carpi, Federico and Danilo De Rossi. "Emg- Based and Gaze- Tracking- Based Man–Machine Interfaces." *International Review of Neurobiology* 86, (2009): 3-21.

Chen, Yingxi and Wyatt S. Newman. "A Human-Robot Interface Based on Electrooculography." In *Robotics and Automation, 2004. Proceedings. ICRA'04. 2004 IEEE International Conference on*, vol. 1, pp. 243-248. IEEE, 2004.

Cho, Chul Woo, Eui Chul Lee, Kang Ryoung Park, and Ji Woo Lee. "Robust Gaze-Tracking Method by using Frontal-Viewing and Eye-Tracking Cameras." *Optical Engineering* 48, no. 12 (2009): 127202-127202.

Drewes, Heiko. "Eye gaze tracking for human computer interaction." PhD diss., Media Informatics Group, LMU Munich, Munich, Germany, 2010.

Gonzalez, Rafael C. and Richard E. Woods. "Digital Image Processing." Prentice-Hall, Upper Saddle River, NJ, USA, 2nd edition. (2002).

Hansen, Dan Witzner, David JC MacKay, John Paulin Hansen, and Mads Nielsen. "Eye Tracking Off the Shelf." In *Proceedings of the 2004 symposium on Eye tracking research & applications*, pp. 58-58. ACM, 2004.

Khalid, Muhammad Bilal, Naveed Iqbal Rao, Intisar Rizwan-i-Haque, Sarmad Munir, and Farhan Tahir. "Towards a Brain Computer Interface using Wavelet Transform

with Averaged and Time Segmented Adapted Wavelets." In *Computer, Control and Communication, 2009. IC4 2009. 2nd International Conference on*, pp. 1-4. IEEE, 2009.

Kübler, Andrea, Boris Kotchoubey, Jochen Kaiser, Jonathan R. Wolpaw, and Niels Birbaumer. "Brain–computer Communication: Unlocking the Locked in." *Psychological Bulletin* 127, no. 3 (2001): 358.

Kubota, Yasutaka, Wataru Sato, Motomi Toichi, Toshiya Murai, Takashi Okada, Akiko Hayashi, and Akira Sengoku. "Frontal Midline Theta Rhythm is Correlated with Cardiac Autonomic Activities during the Performance of an Attention Demanding Meditation Procedure." *Cognitive Brain Research* 11, no. 2 (2001): 281-287.

Lee, Eui Chul, Jin Cheol Woo, Jong Hwa Kim, Mincheol Whang, and Kang Ryoung Park. "A Brain–computer Interface Method Combined with Eye Tracking for 3D Interaction." *Journal of Neuroscience Methods* 190, no. 2 (2010): 289-298.

Lee, Ji Woo, Hwan Heo, and Kang Ryoung Park. "A Novel Gaze Tracking Method Based on the Generation of Virtual Calibration Points." *Sensors* 13, no. 8 (2013): 10802-10822.

Lee, Kwang-Hyuk, Leanne M. Williams, Michael Breakspear, and Evian Gordon. "Synchronous Gamma Activity: A Review and Contribution to an Integrative Neuroscience Model of Schizophrenia." *Brain Research Reviews* 41, no. 1 (2003): 57-78.

Li, Dongheng. "Low-cost eye-tracking for human computer interaction." MS thesis, Iowa State University, Ames, IA, USA, 2006.

Li, Dongheng, Jason Babcock, and Derrick J. Parkhurst. "openEyes: A Low-Cost Head-Mounted Eye-Tracking Solution." In *Proceedings of the 2006 symposium on Eye tracking research & applications*, pp. 95-100. ACM, 2006.

Malmivuo, Jaakko and Robert Plonsey. *Bioelectromagnetism: Principles and Applications of Bioelectric and Biomagnetic Fields.* Oxford, U.K.: Oxford University Press, 1995.

Mantiuk, Radosław, Michał Kowalik, Adam Nowosielski, and Bartosz Bazyluk. "Do-it-Yourself Eye Tracker: Low-Cost Pupil-Based Eye Tracker for Computer Graphics Applications." In *Advances in Multimedia Modeling.* K. Schoeffmann, *et al.,* Eds. Berlin/Heidelberg, Germany: Springer, 2012, pp. 115-125.

Morimoto, Carlos H. and Marcio RM Mimica. "Eye Gaze Tracking Techniques for Interactive Applications." *Computer Vision and Image Understanding* 98, no. 1 (2005): 4-24.

Morimoto, Carlos Hitoshi, David Koons, Arnon Amir, and Myron Flickner. "Pupil Detection and Tracking using Multiple Light Sources." *Image and Vision Computing* 18, no. 4 (2000): 331-335.

Nicolas-Alonso, Luis Fernando and Jaime Gomez-Gil. "Brain Computer Interfaces, a Review." *Sensors* 12, no. 2 (2012): 1211-1279.

Nussbaum, Paul Alton and Rosalyn Hobson Hargraves. "Pilot Study: The use of Electroencephalogram to Measure Attentiveness Towards Short Training Videos." *International Journal of Advanced Computer Science & Applications* 4, no. 3 (2013).

Pfurtscheller, Gert, Brendan Z. Allison, Clemens Brunner, Gunther Bauernfeind, Teodoro Solis-Escalante, Reinhold Scherer, Thorsten O. Zander, Gernot Mueller-Putz, Christa Neuper, and Niels Birbaumer. "The Hybrid BCI." *Frontiers in Neuroscience* 4, (2010).

Pfurtscheller, Gert and Christa Neuper. "Motor Imagery and Direct Brain-Computer Communication." *Proceedings of the IEEE* 89, no. 7 (2001): 1123-1134.

Pineda, Jaime A. "The Functional Significance of Mu Rhythms: Translating “seeing” and “hearing” into “doing”." *Brain Research Reviews* 50, no. 1 (2005): 57-68.

Salabun, Wojciech. "Processing and Spectral Analysis of the Raw EEG Signal from the MindWave." *Przeglad Elektrotechniczny* 90, (2014): 169-174.

Schalk, Gerwin, Dennis J. McFarland, Thilo Hinterberger, Niels Birbaumer, and Jonathan R. Wolpaw. "BCI2000: A General-Purpose Brain-Computer Interface (BCI) System." *Biomedical Engineering, IEEE Transactions On* 51, no. 6 (2004): 1034-1043.

Wolpaw, Jonathan R., Niels Birbaumer, Dennis J. McFarland, Gert Pfurtscheller, and Theresa M. Vaughan. "Brain–computer Interfaces for Communication and Control." *Clinical Neurophysiology* 113, no. 6 (2002): 767-791.

Zhang, Biao, Jianjun Wang, and Thomas Fuhlbrigge. "A Review of the Commercial Brain-Computer Interface Technology from Perspective of Industrial Robotics." In *Automation and Logistics (ICAL), 2010 IEEE International Conference on*, pp. 379-384. IEEE, 2010.

Zhang, Li, Wei He, Chuanhong He, and Ping Wang. "Improving Mental Task Classification by Adding High Frequency Band Information." *Journal of Medical Systems* 34, no. 1 (2010): 51-60.

Zielinski, P. "Opengazer: Open-Source Gaze Tracker for Ordinary Webcams." *Samsung and The Gatsby Charitable Foundation, http://www.inference.phy.cam.ac.uk/opengazer (2007).*